Suppl. Figure S1

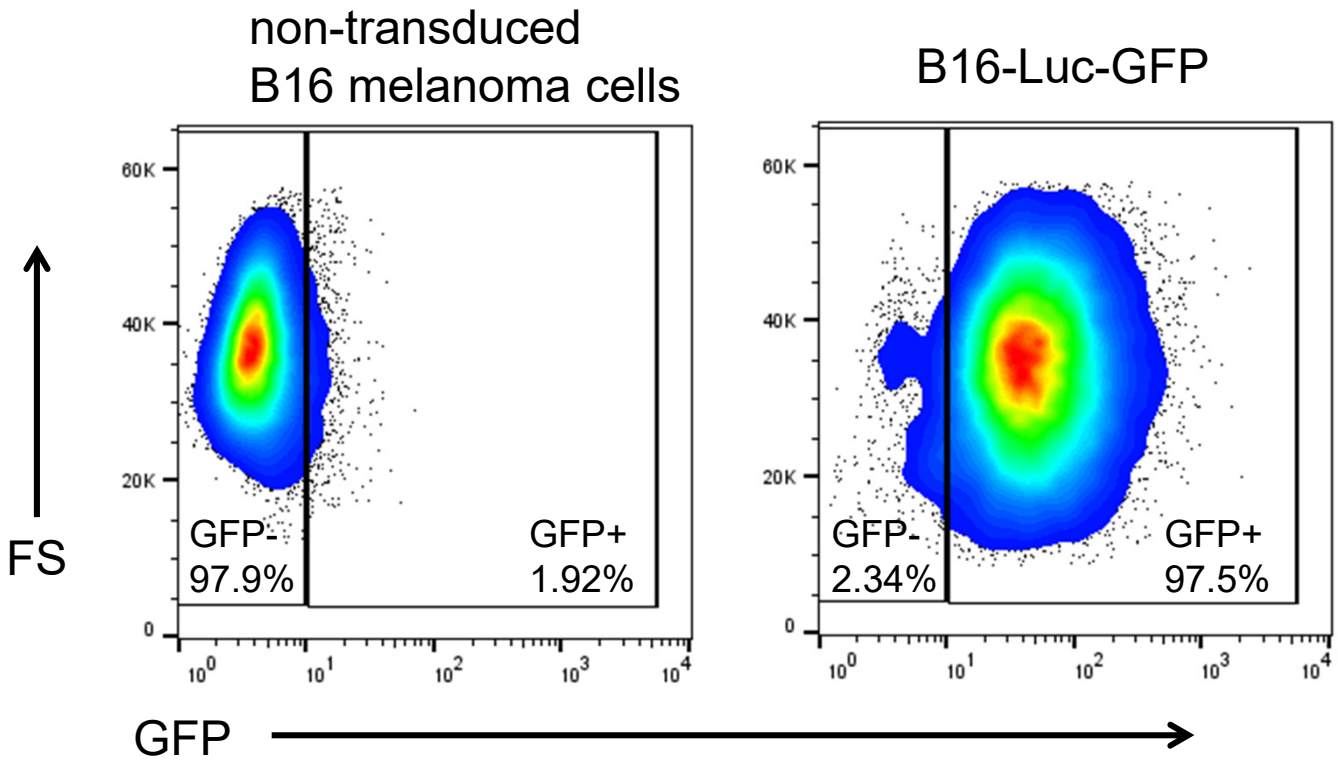

Suppl. Figure S2

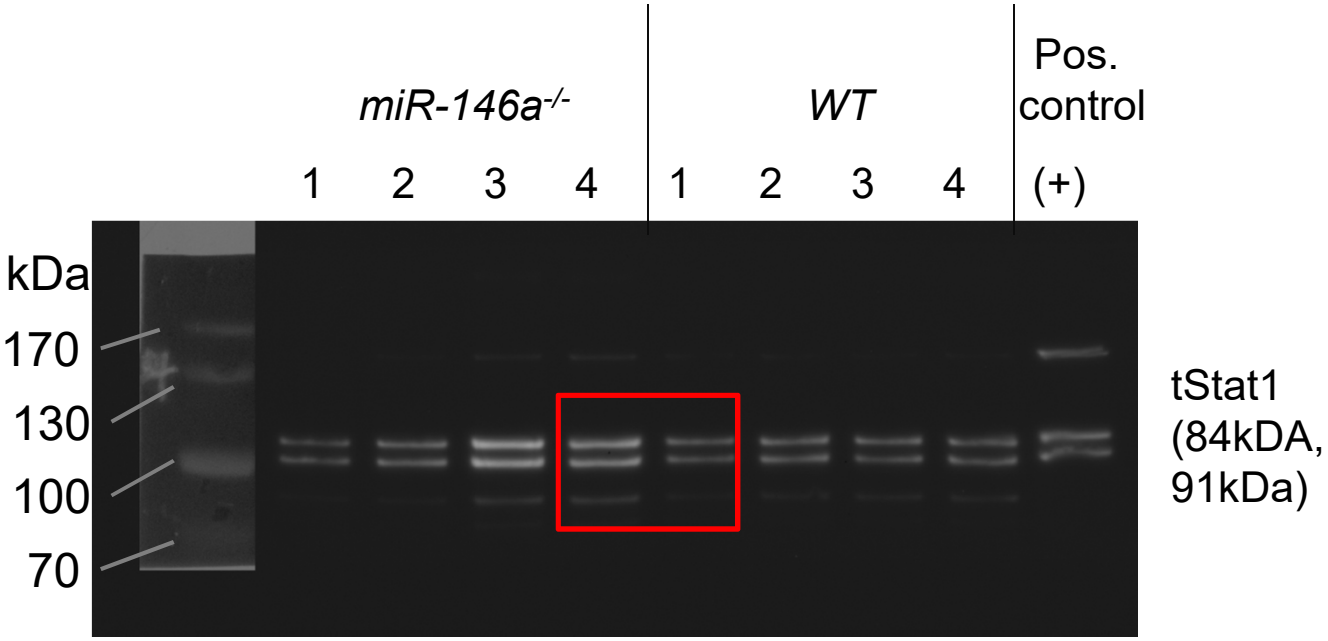

Suppl. Figure S3

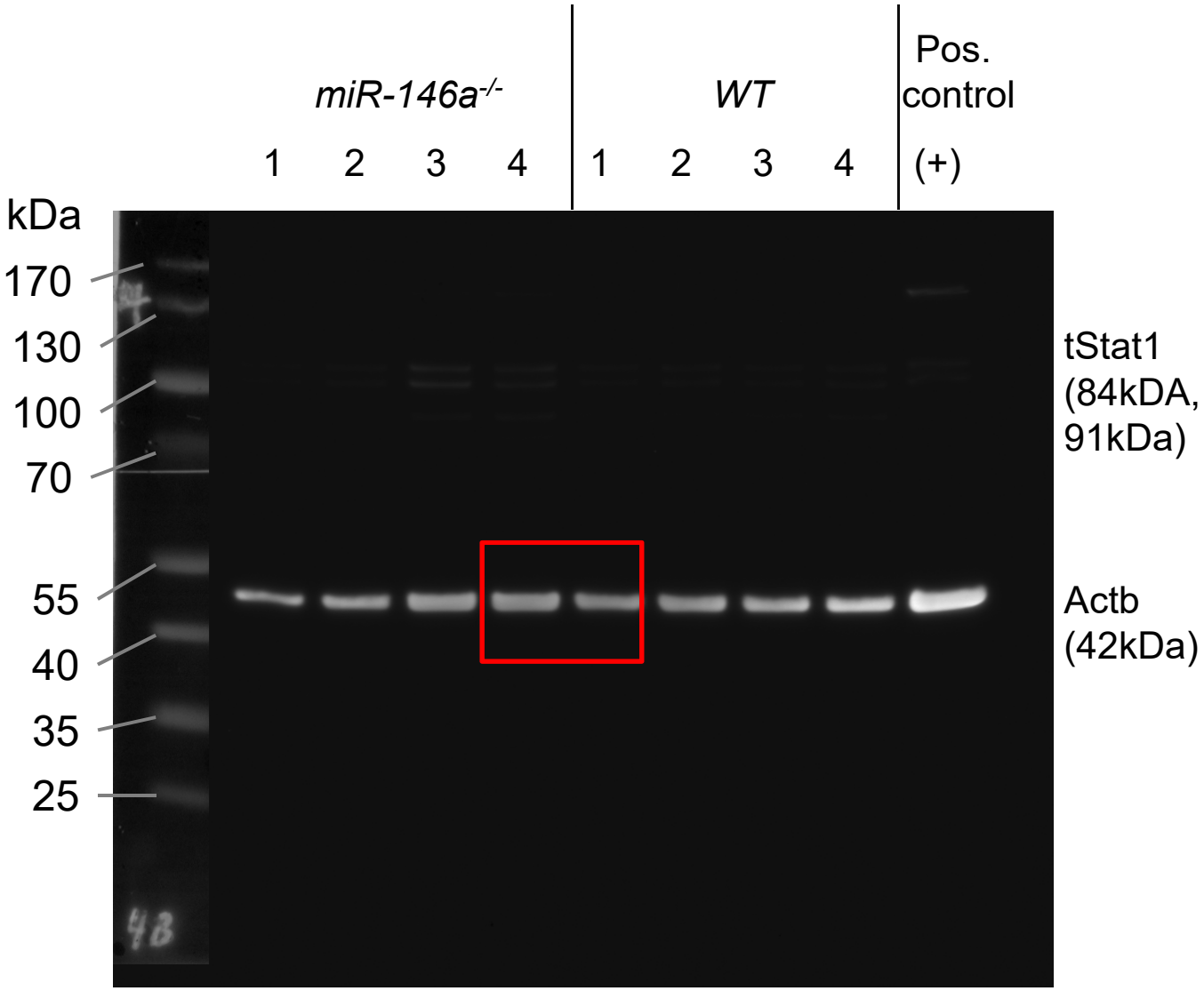

Suppl. Figure S4

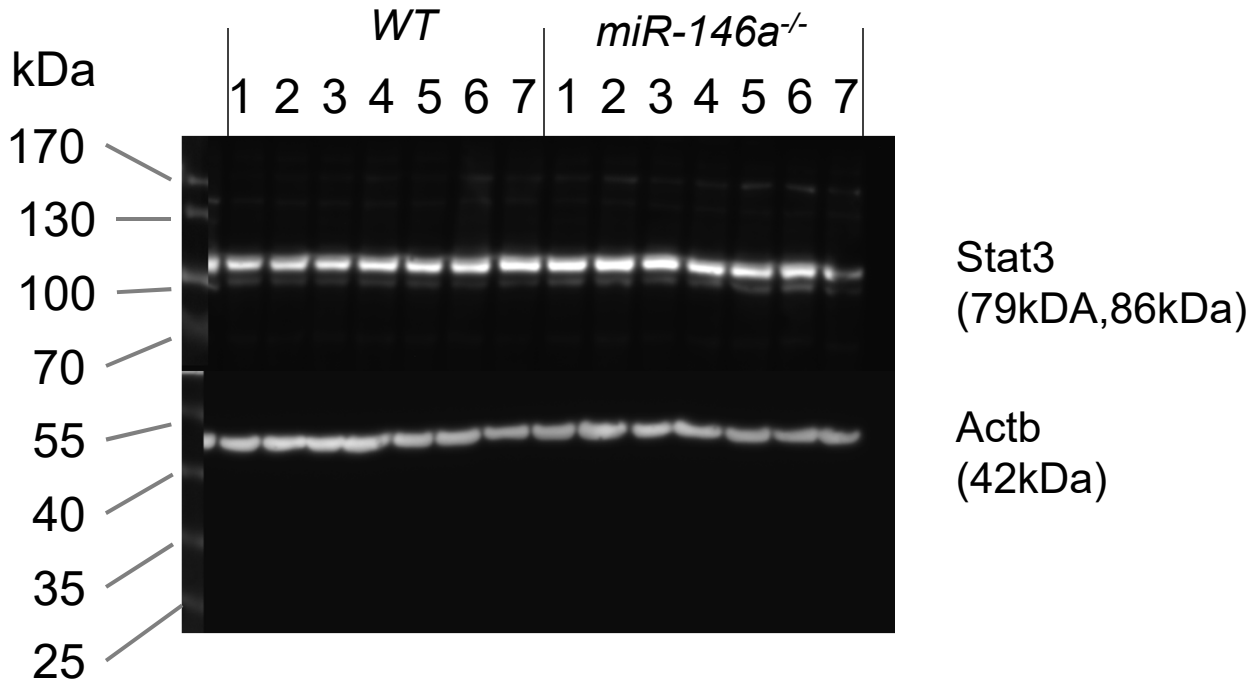

Suppl. Figure S5

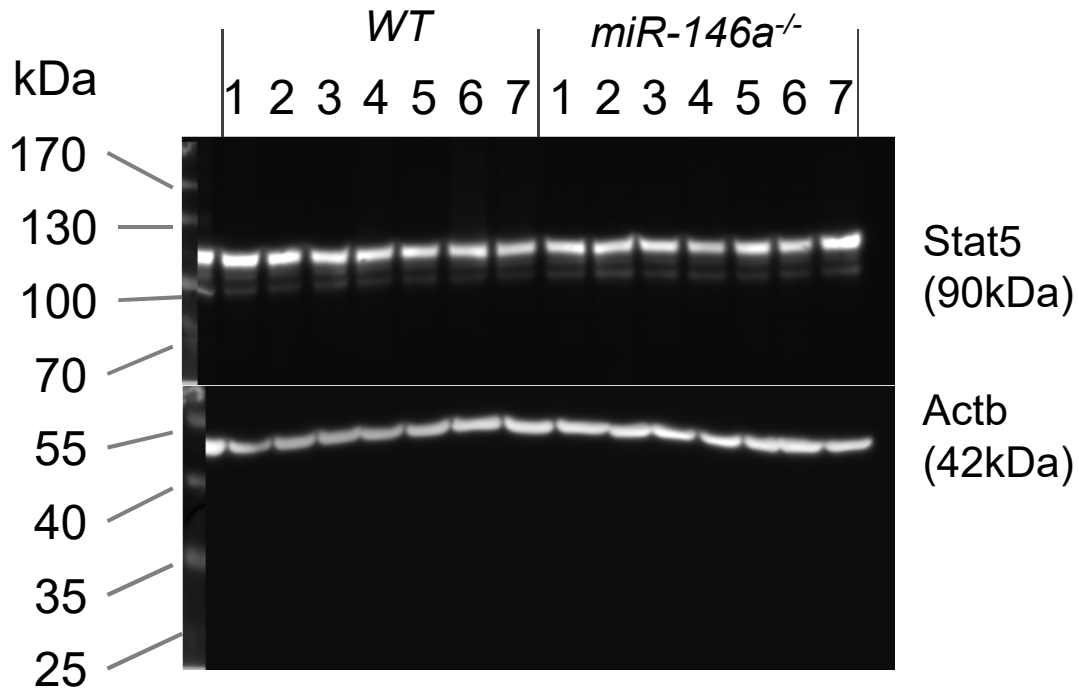

Suppl. Figure S6

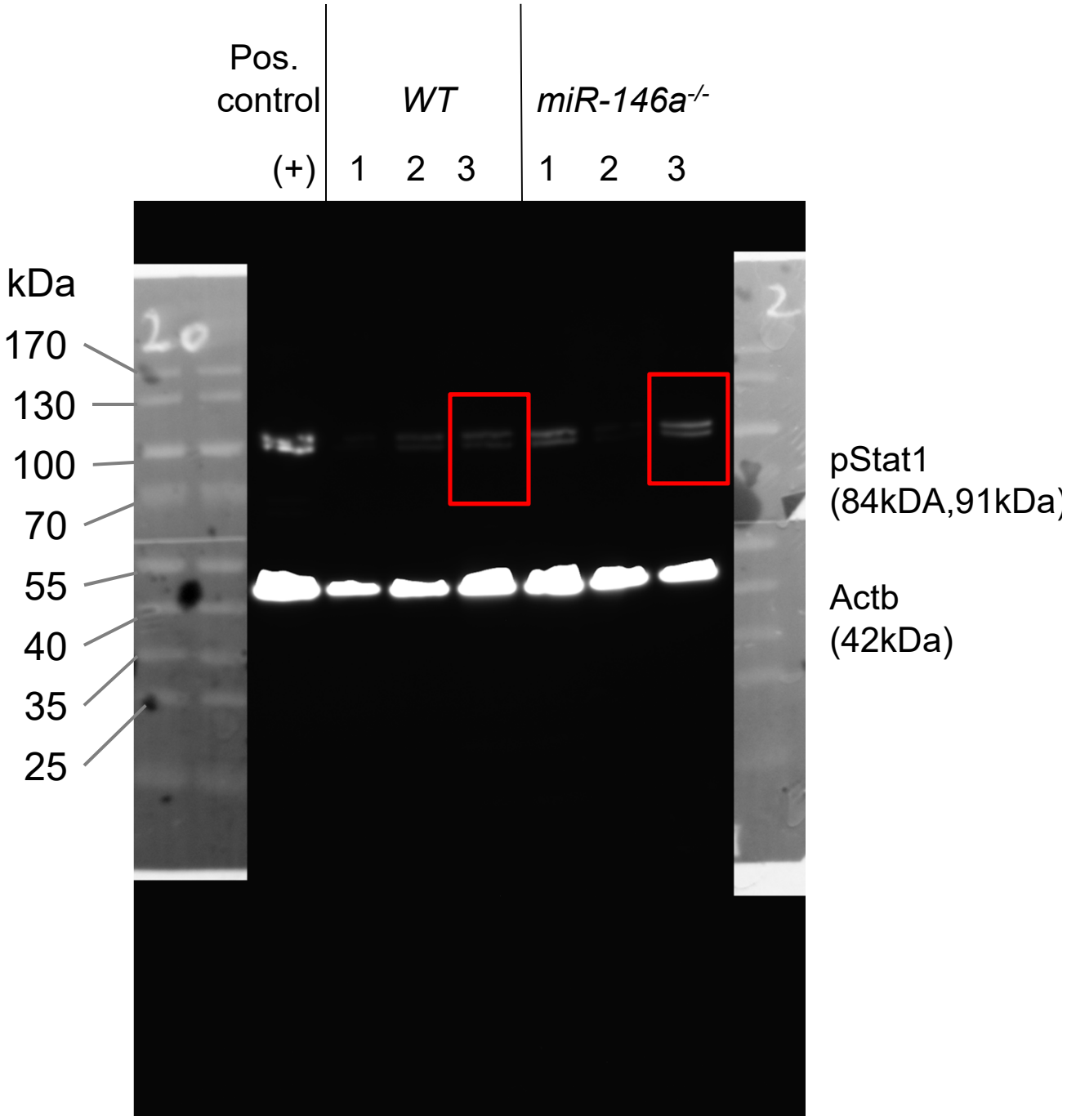

Suppl. Figure S7

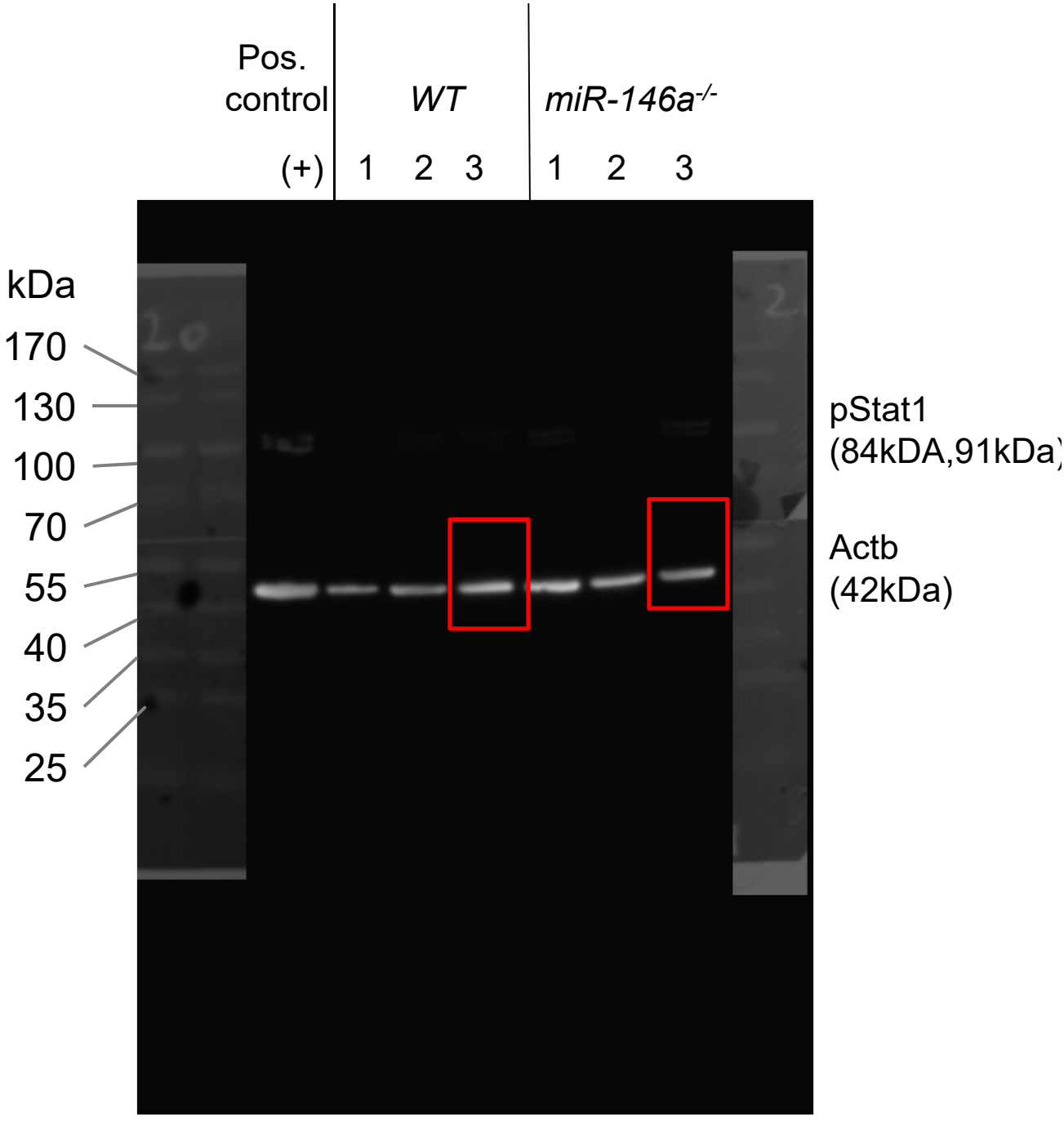

Suppl. Figure S8

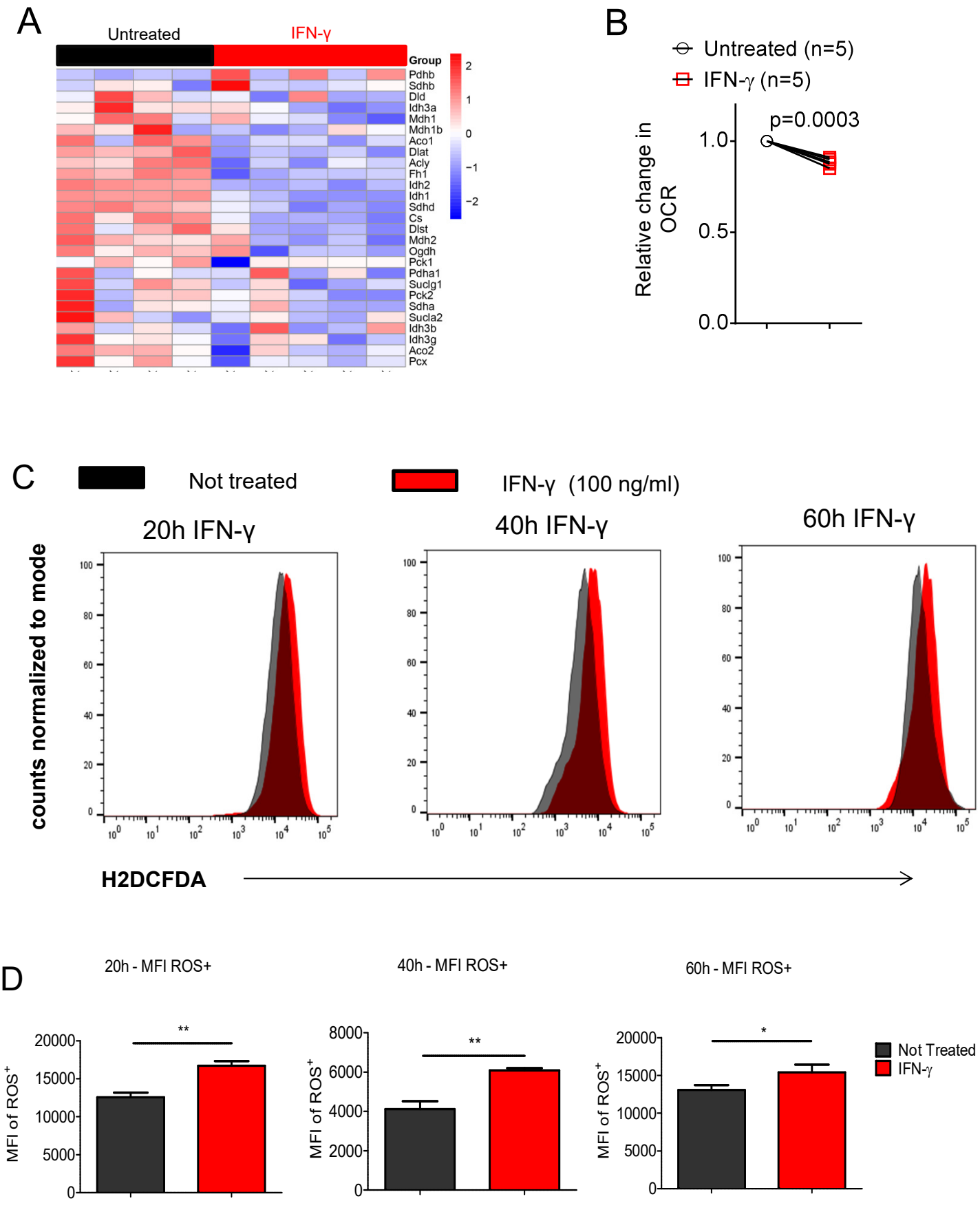

Suppl. Figure S9

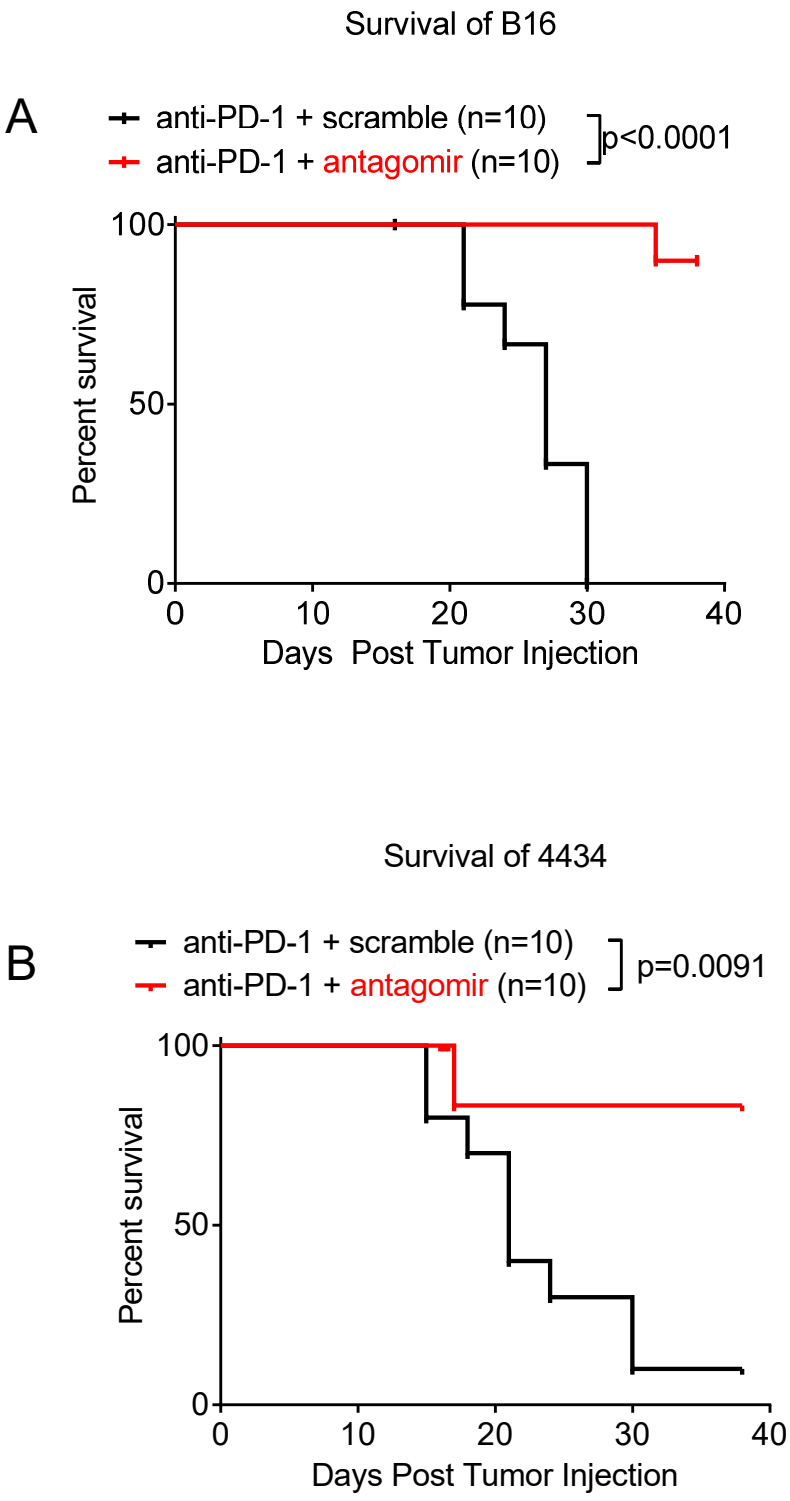

Suppl. Figure S10

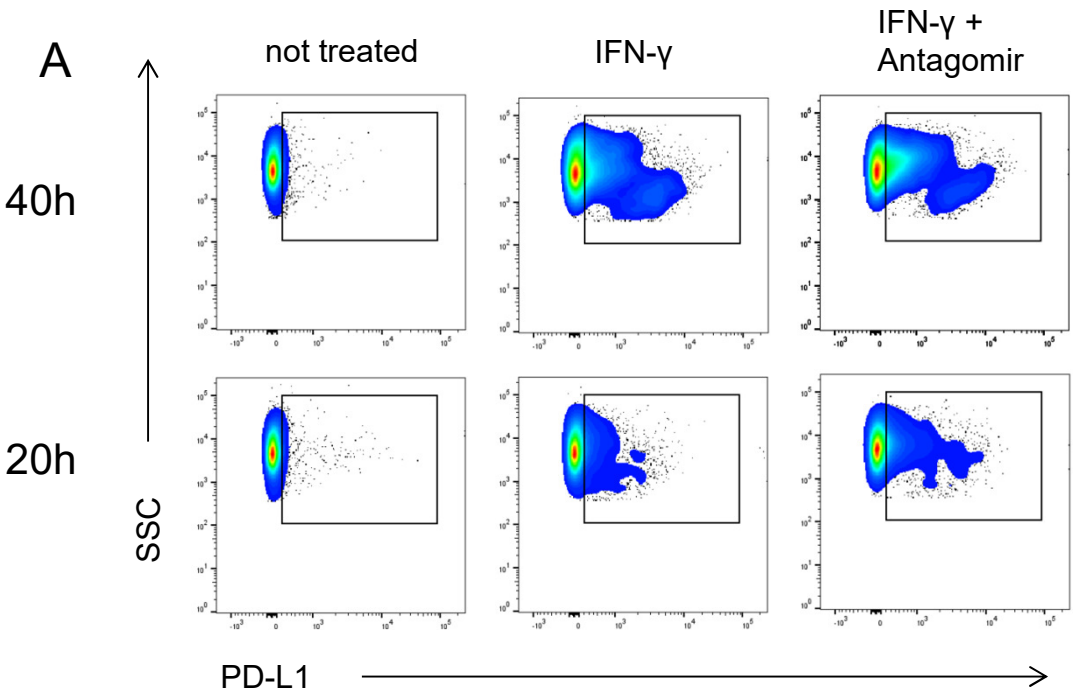

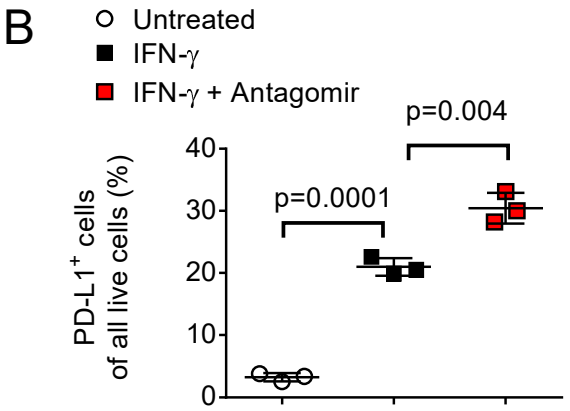

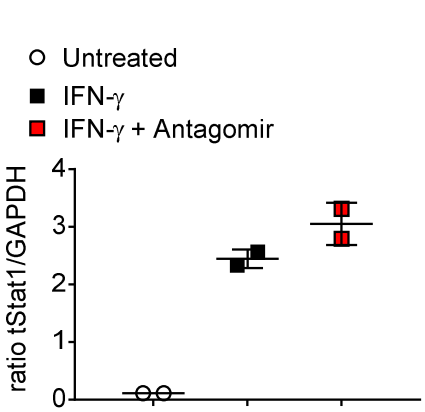

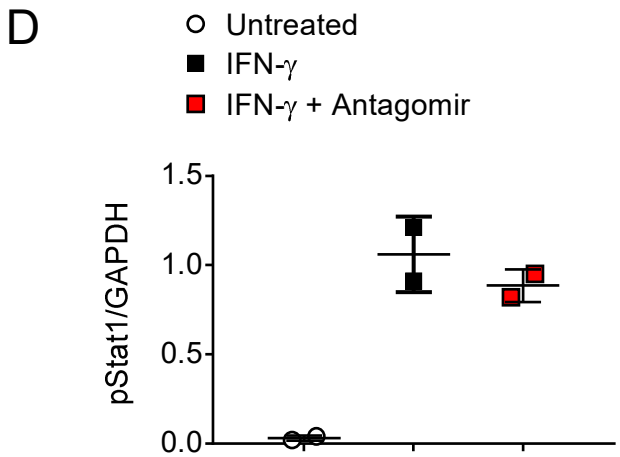

Suppl. Figure S11

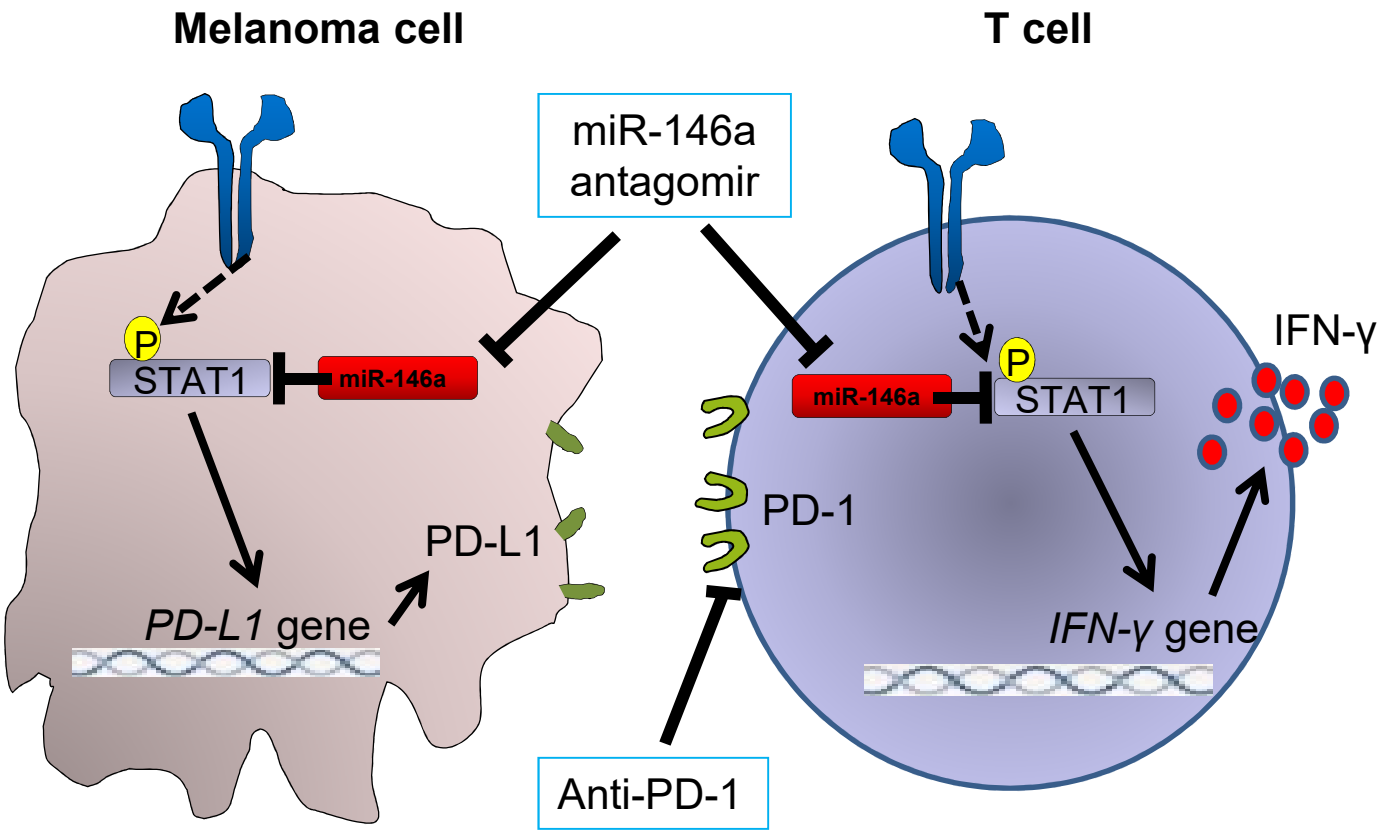

Supplemental Figure Legends:

(S1) Supplemental Figure S1 shows the flow cytometry based analysis of B16 cells transformed with a lentiviral vector with Luc-GFP-neo

The flow cytometry based analysis shows B16 cells transformed with a lentiviral vector with Luc-GFP-neo transgene compared to non-transduced cells. The B16-luc-GFP$^+$ were selected for with 2mg/ml Geneticin. Selection of transduced cells resulted in > 97% GFP+ cells, while the < 2% GFP$^+$ cells in the non-transduced cells could be attributed to autofluorescence.

S2-S7 Supplemental Figures S2-S7 show complete western blot images.

Complete western blot images are displayed.

(S2) CD4$^+$ CD8$^+$ T cells isolated from SLO of WT and *miR-146a*$^{-/-}$ mice on day 20. T lymphocytes were reactivated for 4 hours with PMA and Ionomycin, 10 µg of protein lysate per sample was loaded into the gel. Western blot membrane exposed for 30 min to reveal total-Stat1 protein, both α and β isoforms at ~84 and ~91 kDa, respectively. Total Stat1 protein cropped to red box and depicted in **Fig 3C**.

(S3) Complete PVDF membrane from Figure S2. Image exposed for 30 seconds to reveal β-ACTIN protein loading control from total Stat1 protein blot depicted in **Fig3C**, cropped to red box.

(S4) CD4$^+$ CD8$^+$ T cells isolated from SLO of WT and *miR-146a*$^{-/-}$ mice on day 21. T lymphocytes were reactivated for 4 hours with PMA and Ionomycin, 10 µg of protein lysate per sample was loaded into the gel. Western blot membrane exposed for 30 min to reveal total-Stat3, both Stat3-α and -β isoforms at 79 and 86kDa. Lower sections of each membrane were exposed for 30 seconds to reveal β-actin protein loading control**.** Each band represents CD4$^+$ CD8$^+$ T cells isolated from a separate mouse.

(S5) $CD4^+$ $CD8^+$ T cells isolated from SLO of WT and *miR-146a*$^{-/-}$ mice on day 21. T lymphocytes were reactivated for 4 hours with PMA and Ionomycin, 10 µg of protein lysate per sample was loaded into the gel. Western blot membrane exposed for 30 min to reveal Stat5 at 90kDa respectively. Lower sections of each membrane were exposed for 30 seconds to reveal β-actin protein loading control**.** Each band represents $CD4^+$ $CD8^+$ T cells isolated from a separate mouse.

(S6) $CD4^+$ $CD8^+$ T cells isolated from SLO of WT and *miR-146a*$^{-/-}$ mice on day 24. T lymphocytes were restimulated for 4 hours with PMA and Ionomycin, 4µg of protein lysate per sample was loaded into the gel. Western blot membrane exposed for 3 min to reveal Phosphorylated-Stat1 protein at Tyr701, antibody detected both α, β isoforms at 84 and 91 kDa, respectively. Positive controls were WT dendritic cells stimulated with LPS for 6 hours. Image was cropped to red boxes and depicted in **Fig 3E**.

(S7) Western blot membrane from **S3**, exposed for 30 seconds to reveal β-actin protein loading control. Image was cropped to red boxes and depicted in **Fig3E**.

(**S8**) **Supplemental Figure S8 shows the impact of IFN gamma on melanoma cells with respect to gene expression, OCR and ROS production**.

A. Heatmap ("Z-score intensity") of genes involved Tricarboxylic Acid Cycle of B16 melanoma cells. Where indicated cells were treated with IFN-γ at a concentration of 100ng/ml for 40 hours.
B. Pooled Seahorse assay data depicting the basal oxygen consumption rate (OCR) of B16 cells treated for 40 hours with 100ng/ml IFN-γ paired to untreated control, 2- tailed one sample *t* test was performed for significance.
C. Flow cytometry histograms of H2DCFDA intensity showing ROS production in melanoma cells exposed to 100ng/ml IFN-γ for the indicated time periods of 20, 40, 60 hours.
D. Quantification of pooled ROS production analyses shown in S8C.

(S9) Supplemental Figure S9 shows the effect of prolonging combination therapy regimen in melanoma bearing mice

A. WT mice injected with B16.F10 luc^{+} melanoma cells were treated as described in the Suppl. methods section. Kaplan-Meier curve reveals survival benefit of prolonged exposure to miR-146a inhibition in combination with anti-PD-1 therapy.
B. Survival curves of WT mice injected with 4434 melanoma cells, then treated with prolonged regimen of anti-PD-1 antibody alone or in combination with miR-146a inhibition.

(**S10**) **Supplemental Figure S10 shows the combined effects of IFN-γ and miR-146a inhibition on melanoma cells *in vitro.***

A. PD-L1 levels expressed on the surface of melanoma cells after 20h or 40h incubation with IFN-γ (100ng/ml) or combination IFN-γ and miR-146a inhibitor (60nmol) compared to untreated control melanoma cells measured via flow cytometry.
B. Percent of PD-L1^{+} of melanoma cells treated for 40h with IFN-γ alone or in combination with miR-146a inhibitor.
C. Ratio of total Stat1 protein to GAPDH in melanoma cells treated with IFN-γ alone or in combination with miR-146a inhibitor.
D. Ratio of phosphorylated Stat1 to GAPDH in melanoma treated as above.

(**S11**) **Supplemental Figure S11 shows the proposed mechanism of action.**

miR-146a targets STAT1 which reduces activity of the STAT1 / IFN-γ axis. Therapeutic targeting of miR-146a increases IFN-γ, which has beneficial effects by reducing melanoma cell proliferation, migration and metabolic activity. However, IFN-γ also leads to increased PD-L1 expression, which can be blocked by anti-PD1 checkpoint blockade leading to the synergism of miR-146a antagomir and anti-PD1 immunotherapy.

Author contributions

J.M. helped to develop the concept, designed experiments, performed experiments, analyzed the data and helped to write the manuscript. N.S., H.A., K.H., D.S., and M.F. helped to perform experiments and analyze data, M.B. and G.A. analyzed microarray data. D.P. performed microarrays, A.S.G. analyzed IHC stains of human melanoma samples. W.M. , S.D., and H.D. helped with experiments. F.M. provided human melanoma samples and patient data. R.Z. developed the overall concept, supervised the experiments, discussed the data and wrote the manuscript.

Supplementary Materials and Methods:

Extension of *in vivo* antibody and oligonucleotide inhibitor treatment

WT mice injected on day 0 with $1x10^4$ B16.F10 luc^+, or in another model $2x10^5$ 4434 melanoma cells in the tail vein, then received 200µg anti-PD-1 antibody, i.p. on days 1, 4 8, 16, 22, 28, and 32. Control mice were treated in parallel with 200µg Armenian hamster isotype control purchased from BioXcell, (cat# BE0091). Oligonucleotides inhibiting miRNA-146a (ThermoFisher mirVana™ miRNA Inhibitor, Cat#: 4464088 ID: MH10722) or scramble controls (ThermoFisher mirVana™ miRNA Inhibitor, Negative Control #1, Cat#: 4464079) were administered via tail vein injections on days 5, 9 and 16. *In vivo*-jetPEI® (Polyplus, cat# 201-50G), facilitated *in vivo* delivery of oligonucleotides across cell membranes, for 60µg of oligonucleotides injected in 200µl volume of 5% Glucose/*in vivo*-jet-PEI, according to product description.

Sea horse assay

Seahorse XFp miniplates were seeded with $1x10^4$ B16 melanoma cells per well. Oxygen consumption rates (OCR) of was measured in XF media (non-buffered RPMI 1640 containing 25 mM glucose, 2mM L-glutamine, and 1 mM sodium pyruvate) under basal conditions and in response to 1 µM oligomycin, 1.5 µM fluoro-carbonyl cyanide phenylhydrazone (FCCP) and 100 nM rotenone + 1 µM antimycin A, (Sigma) using an 8-well Seahorse XFp Analyzer (Seahorse Bioscience) as previously described (1,2). After metabolism assay, protein content of each well

was measured via BCA. The results of the metabolism were then normalized to µg protein per well.

Reactive Oxygen Species (ROS) Measurement

B16 melanoma cells were incubated for 20, 40, and 60 hours with and without IFN-γ (100ng/ml). In the final hour of incubation cells were gently washed with PBS, then incubated at 37°C with 1.16µg/ml 2,7 dichlorofluoroscin diacetate (H2DCFDA) in PBS for one hour. Melanoma cells were then analyzed via flow cytometry for the hourly production rate of ROS.

Effect of miR-146a inhibition on IFN-γ induced melanoma, *in vitro*

B16 melanoma cells were seeded, 200,000 cells/well in a 6 well plate, then treated with 100ng/ml IFN-γ alone, or in combination with 60nmol Antagomir miR-146a in lipofectamine for 20 and 40 hours, and compared with untreated melanoma cells for PD-L1 surface expression via flow cytometry, and protein expression via western blot.

1. van der Windt GJ, Everts, B., Chang, C.H., Curtis, J.D., Freitas, T.C., Amiel, E., Pearce, E.J., Pearce, E.L. Mitochondrial respiratory capacity is a critical regulator of CD8+ T cell memory development. Immunity 2012;36:68-78.
2. Mathew NR, Baumgartner, F., Braun, L., David O´Sullivan, Thomas S, Waterhouse M, Müller TA, Hanke K, Taromi S, Apostolova P, Illert AL, Melchinger W, Duquesne S, Schmitt-Graeff A, Osswald L, Yan K-L., Weber A, Tugues S, Spath S, Pfeifer D, Follo M, Claus R, Lübbert M, Rummelt C, Bertz H, Wäsch R, Haag J, Schmidts A, Schultheiss M, Bettinger M, Thimme R, Ullrich E, Tanriver Y, Vuong GL, Arnold R, Hemmati P, Wolf D, Ditschkowski M, Jilg C, Wilhelm K, Leiber C, Gerull S, Halter J, Lengerke C, Pabst T, Schroeder T, Kobbe G, Rösler W, Doostkam S, Meckel S, Stabla K, Metzelder SK, Halbach S, Brummer T, Hu Z, Dengjel J, Hackanson B, Schmid C, Holtick U, Scheid C, Spyridonidis A, Stölzel F, Ordemann F, Müller LP, Sicre-de-Fontbrune F, Ihorst G, Kuball J, Ehlert JE, Feger D, Wagner EV, Cahn JY, Schnell J, Kuchenbauer F, Bunjes D, Chakraverty R, Richardson S, Gill S, Kröger N, Ayuk F, Vago L, Ciceri F, Müller AM, Kondo T, Teshima T, Klaeger S, Kuster B, Kim D, Weisdorf D, van der Velden W, Dörfel D, Bethge W, Hilgendorf I, Hochhaus A, Andrieux G, Börries M, Busch H, Magenau J,

Reddy P, Labopin M, H. Antin J, Henden AS, Hill GR, Kennedy GA, Bar M, Sarma A, McLornan D, Mufti G, Oran B, Rezvani K, Sha O, Negrin RS, Nagler A, Prinz M, Burchert A, Neubauer A, Beelen D, Mackensen A, von Bubnoff N, Herr W, Becher B, Socié G, Caligiuri MA, Ruggiero E, Bonini C, Häcker G, Duyster J, Finke J, Pearce E, Blazar BR, Zeiser R. Sorafenib promotes graft-versus-leukemia activity in mice and humans through IL-15 production in FLT3-ITD mutant leukemia cells. Nature medicine 2018;24:282-91.